

# Optimization for Maximizing Sum Secrecy Rate in SWIPT-enabled NOMA Systems

Jie Tang, *Senior Member, IEEE*, Tuwang Dai, Manman Cui, Xiuyin Zhang, *Senior Member, IEEE*, Arman Shojaefard, *Member, IEEE*, Kai-Kit Wong, *Fellow, IEEE* and Zan Li, *Senior Member, IEEE*

**Abstract**—In this paper, we study secrecy simultaneous wireless information and power transfer (SWIPT) in downlink non-orthogonal multiple access (NOMA) systems comprising a base station (BS), multiple information receivers (IRs), and multiple energy receivers (ERs) that have potential to wiretap the IRs. The goal of this paper is to maximize the sum secrecy rate (SSR) of the system subject to the individual IR's minimum data rate requirement and the individual ER's minimum harvested energy requirement. The corresponding problem involves resource allocation via max-min function, which is non-convex and difficult to solve directly. In order to tackle this, we first transform the original non-convex problem to a sequence of convex sub-problems which can be solved simultaneously. Hence, a closed-form solution of the optimal power allocation policy is derived based on the Karush-Kuhn-Tucker (KKT) conditions. Numerical results validate the theoretical findings and demonstrate that significant performance gain over the orthogonal multiple access (OMA) scheme in terms of SSR can be achieved by the proposed algorithm in a SWIPT-enabled NOMA system.

**Index Terms**—Non-orthogonal multiple access (NOMA), physical layer security, simultaneous wireless information and power transfer (SWIPT).

## I. INTRODUCTION

Orthogonal frequency division multiple access (OFDMA) is the de facto multiple-access technology in the downlink of existing fourth generation (4G) wireless networks. In OFDMA systems, different users are allocated orthogonal frequency resources, which can effectively mitigate inter-user interference but in turn would restrict the system spectrum efficiency. On the other hand, due to the extensive popularization of smart devices and the rapid development of Internet of Thing (IoT) technology, it is foreseen that the data traffic is anticipated to increase by 1000-fold by 2020 for the fifth generation

(5G) networks, and the future communication networks will be required to support massive connected devices [1]. Given the fact that the above requirements are far beyond the range of 4G's capability, non-orthogonal multiple access (NOMA), for its superiority on substantially enhancing the system spectrum efficiency and accommodating massive connectivity, has received considerable attention as a promising candidate technology for 5G [2]–[4].

Different from the conventional orthogonal multiple access (OMA), NOMA is capable of serving multiple users by exploiting the power-domain for multiple access with superposition coding, and thus it can further improve the system spectrum efficiency. Sharing the same spectrum among users leads to a high mutual interference when decoding information. However, by employing successive interference cancellation (SIC) at the receiver, the information can be correctly decoded and thus improve the throughput of the system [3]. As a result, NOMA with the non-orthogonal resource allocation and SIC may achieve significance interference reduction which, together with facilitating massive connectivity, translates to higher multi-user capacity [4]. In addition, results in [5] reveal that the system-level performance of NOMA is superior to that of OMA in terms of the degree of proportional fairness, the overall cell throughput and cell-edge user throughput. Based on this study, NOMA has attracted great interest [6]–[9]. For instance, to ensure fairness among downlink users in NOMA systems, the authors in [6] developed low-complexity bisection-based power iterative algorithms with both instantaneous channel state information (CSI) and average CSI at the transmitter. With the objective of achieving a balance between user fairness and capacity, the authors in [7] proposed a joint optimization of the sub-channel assignment and power allocation in the downlink NOMA systems. Compared to the conventional NOMA with fixed power allocation, authors in [8] proposed a novel dynamic power allocation scheme so as to offer more flexibility in realizing various tradeoffs between the fairness and throughput of the NOMA systems. Considering the impact of the channel estimation error, the authors in [9] proposed a joint user scheduling and power allocation scheme to improve the energy efficiency of the NOMA system with imperfect CSI. Furthermore, due to the distinct advantage concerning spectral efficiency, NOMA has been linked with some other well-known communication networks such as relay networks [10], multiple-input single-output (MISO) networks [11] and multiple-input multiple-output (MIMO) networks [12].

Meanwhile, 5G use cases such as automation factory and

This work has been supported in part by the National Natural Science Foundation of China under Grant 61601186, in part by the Natural Science Foundation of Guangdong Province under Grant 2017A030313383, in part by the Guangzhou Science Technology and Innovation Commission under Grant 201707010159.

J. Tang is with the School of Electronic and Information Engineering, South China University of Technology, and with the State Key Laboratory of Integrated Services Networks, Xidian University, China. (e-mail: eej-tang@scut.edu.cn).

T. Dai, M. Cui and X. Zhang are with the School of Electronic and Information Engineering, South China University of Technology, China. (e-mail: 1075483540@qq.com; emma2012\_scut@163.com; zhangxiuyin@hotmail.com).

A. Shojaefard and K.-K. Wong are with the Department of Electronic and Electrical Engineering, University College London, London, United Kingdom. (e-mail: a.shojaefard@ucl.ac.uk; kai-kit.wong@ucl.ac.uk).

Z. Li is with the State Key Laboratory of Integrated Services Networks, Xidian University, China. (e-mail: zanli@xidian.edu.cn).

Corresponding author: Manman Cui.

smart city require long life battery to support the demand of high data rate services. Recent progress in the research on wireless power transfer (WPT) provides a new possibility for improving the lifespan of energy-constrained wireless devices [13]. Furthermore, it is known that the radio frequency (RF) signals carry both information and energy, which makes it possible to combine WPT and wireless information transmit (WIT) in wireless systems. Motivated by this, an advanced technology named simultaneous wireless information and power transfer (SWIPT), has emerged recently, aiming to achieve the parallel transmission of information and energy. Based on this idea, an information-theoretic study on SWIPT was first investigated in [14]. Ever since SWIPT has attracted great interest recently, e.g. in the context of relay networks [15], OFDMA systems [16], MISO systems [17], [18] and MIMO systems [19], [20]. More specifically, the works in [15] proposed two relaying protocols to enable the wireless energy harvesting (EH) and information decoding (ID) in the wireless amplify-and-forward relaying network. In [16], the authors studied the weighted sum rate maximization problem in multiuser SWIPT OFDMA systems under a set of harvested energy and transmission power constraints. In MIMO broadcast systems, the authors in [19] proposed a joint antenna selection and transmit covariance matrix optimization for SWIPT in order to maximize the achievable rate of the ID receiver. In [17], the authors developed a joint information and energy transmit beamforming design to maximize the weighted sum-power harvested in a SWIPT-enabled multiuser MISO broadcast system. Due to the immense potential of SWIPT and NOMA, the combination of these two techniques has attracted great interest to explore more reliable and more efficient networks for 5G networks [21]–[23]. In [21], the authors investigated the integration of SWIPT and two cooperative networks, i.e., NOMA with fixed power allocation and cognitive radio inspired NOMA, and analyzed the effect of power allocation on their outage performance. The work in [22] demonstrated that the integration of SWIPT into NOMA can improve the reliability of the far NOMA users' without draining the near users batteries. In [23], the authors employed a hybrid time-switching/power-splitting SWIPT architecture for a two-user MISO-NOMA system to improve the performance of the cell-edge users in terms of outage probability and diversity gain.

Nevertheless, the broadcast characteristics of wireless transmission which makes the information vulnerable to eavesdropping, poses a challenge to realize robust secure transmission for wireless networks, especially in SWIPT systems. Due to the practical requirements, energy receivers (ERs) generally locate closer to the transmitter than information receivers (IRs), thus it is more likely to cause the information security problem since ERs with better channel conditions would be prone to wiretap the information transmitted to IRs. Based on that, the concept of physical layer security, which can efficiently prevent information from eavesdropping by utilizing the uniqueness and reciprocity of the fading channels, has attracted extensive attention in both academia and industry [24]–[28]. As demonstrated in [24], secrecy communication would be achievable when the legitimate channel condition is better than the wiretapping channel condition. Based on this theorem,

the work in [25] proposed a joint power and subcarrier allocation to simultaneously maximize the average aggregate information rate of multiple normal users and guarantee the basic average secrecy rate requirements of multiple secrecy users. In [26], a joint information and energy beamforming strategy has been proposed to maximize the harvested sum-energy by multiple ERs subject to a predefined secrecy rate constraint at the IR. It has been extended in [27] to the case of a MISO-SWIPT system comprising multiple IRs and ERs. In particular, a joint information and artificial noise (AN) beamforming design was proposed for the sum secrecy rate (SSR) maximization. Besides, the SSR maximization problem was studied for NOMA systems with power allocation in [28].

### A. Motivation and Contribution

In contrast to the existing literature, which focuses on optimizing the SWIPT-enabled NOMA systems without eavesdropping, e.g. outage performance [21]–[23], transmission rate [29]–[31], and harvested energy [32], in this paper, we study the physical layer security of SWIPT-enabled NOMA systems. In particular, we investigate the SSR maximization problem by means of downlink power allocation, subject to the minimum data rate requirements of the IRs and the minimum harvested energy requirements of the ERs. The main contributions of this paper can be summarized as follows.

- The formulated SSR maximization problem involves resource allocation via the max-min function, and thus is non-convex and difficult to solve directly.
- To overcome the non-convexity of the primal SSR maximization problem, we transform the original non-convex problem into a sequence of convex sub-problems which can be solved simultaneously. We then develop an efficient power allocation algorithm where the corresponding closed-form expressions are derived by invoking the Karush-Kuhn-Tucker (KKT) conditions.
- Numerical simulation results validate the theoretical findings and demonstrate that significant performance gains in terms of SSR can be achieved by adopting the proposed algorithm, and hence showcases the promising potential from the integration of SWIPT technology in NOMA systems.

### B. Organization

The rest of this paper is organized as follows. In Section II, we describe the SWIPT-enabled NOMA system and present the formulation of the SSR maximization problem under consideration. In Section III, we transform the original non-convex problem into a sequence of convex sub-problems, and develop an efficient power allocation algorithm. In Section IV, the numerical results are presented to assess the validity of the theoretical findings. Finally, we conclude this paper in Section V.

## II. SYSTEM MODEL AND PROBLEM FORMULATION

In this section, we first present the SWIPT-enabled NOMA system model and then mathematically formulate the SSR maximization problem.

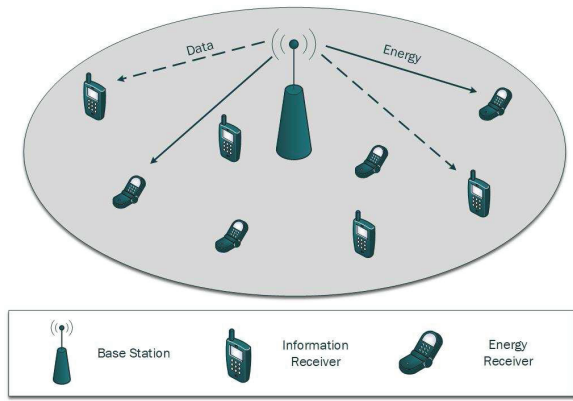


Fig. 1. A downlink SWIPT-enabled NOMA system.

### A. System model

As shown in Fig. 1, we consider a downlink SWIPT-enabled NOMA system, consisting of one base station (BS) with a single antenna,  $M$  single-antenna IRs and  $K$  single-antenna ERs. In practise, since the ERs usually have a shorter access distance to the BS than IRs, it enables ERs not only to harvest energy but also attempt to wiretap information from the received signals. Therefore, all the ERs are potential eavesdroppers for each IR. It is assumed that the channel state information (CSI) of all receivers is perfectly known at the BS. Here we consider the effects of large-scale fading and small-scale fading during the transmission process. The channel coefficients from the BS to the  $m$ -th IR and the  $k$ -th ER are denoted by  $h_m (m \in \{1, 2, \dots, M\})$  and  $g_k (k \in \{1, 2, \dots, K\})$ , respectively. More specifically, we define  $h_m = d_m^{-\frac{\alpha}{2}} v_m$  and  $g_k = d_k^{-\frac{\alpha}{2}} v_k$ , where  $d_m$  and  $d_k$  are the distances from the BS to  $m$ -th IR and the  $k$ -th ER, respectively,  $\alpha$  is the path loss exponent,  $v_m$  and  $v_k$  are the Rayleigh fading coefficients from the BS to  $m$ -th IR and the  $k$ -th ER, respectively.

Utilizing the principle of NOMA, the BS would broadcast a linear combination of  $M$  signals to the IRs, and the transmitted superimposed signal can be expressed as  $\sum_{m=1}^M \sqrt{a_m P} x_m$ , where  $a_m P$  denotes the transmit power of the  $m$ -th IR's signal with power allocation coefficient  $a_m$  subject to  $\sum_{m=1}^M a_m \leq 1$ ,  $P$  is the total transmit power of the BS, and  $x_m$  is the message symbol to the  $m$ -th IR.

Thus the received signal at the  $m$ -th IR can be formulated as

$$y_m = h_m \sum_{m=1}^M \sqrt{a_m P} x_m + n_m, \forall m. \quad (1)$$

where  $n_m$  is the additive white gaussian noise (AWGN) with zero mean and variance  $\sigma^2$ . Similarly, the signal received at the  $k$ -th ER, which acts as a potential eavesdropper, can be expressed as

$$y_k = g_k \sum_{m=1}^M \sqrt{a_m P} x_m + n_k, \forall k. \quad (2)$$

where  $n_k$  is the AWGN with zero mean and variance  $\sigma^2$ . Then

the harvested energy at the  $k$ -th ER can be denoted by

$$E_k^{ER} = \eta P |g_k|^2 \sum_{m=1}^M a_m, \forall k. \quad (3)$$

where  $\eta$  ( $0 < \eta \leq 1$ ) is the energy conversion efficiency of the ERs.

### B. Sum secrecy rate of the system

Similar to [28], without loss of generality, we sort the channel gains as  $0 < |h_1|^2 \leq |h_2|^2 \leq \dots \leq |h_M|^2$  and  $0 < |g_1|^2 \leq |g_2|^2 \leq \dots \leq |g_K|^2$ . After receiving signals, all the IRs are applying SIC to decode their own signal. Particularly, the  $m$ -th IR would first detect the  $i$ -th IR's message with  $i < m$ , and then remove this message from its observed mixture in a successive way; while for the  $i$ -th IR with  $i > m$  the message would be treated as noise. Therefore, the achievable rate of the  $m$ -th IR can be derived as follows:

$$R_m^{IR} = \log_2 \left( 1 + \frac{P |h_m|^2 a_m}{P |h_m|^2 \sum_{i=m+1}^M a_i + \sigma^2} \right), \forall m. \quad (4)$$

Meanwhile, the achievable rate of the  $k$ -th ER wiretapping the  $m$ -th IR can be expressed as

$$R_{k,m}^{ER} = \log_2 \left( 1 + \frac{P |g_k|^2 a_m}{P |g_k|^2 \sum_{i=m+1}^M a_i + \sigma^2} \right), \forall k. \quad (5)$$

Thereby, the achievable secrecy rate of the  $m$ -th IR under the  $k$ -th ER eavesdropping and the SSR of the system can be, respectively, given by

$$R_{k,m}^s = [R_m^{IR} - R_{k,m}^{ER}]^+, \quad (6)$$

$$R_s = \sum_{m=1}^M \min_k R_{k,m}^s. \quad (7)$$

where  $[x]^+ \triangleq \max(0, x)$ . From above, the achievable secrecy rate is the IR's achievable rate minus the wiretap rate, when  $R_m^{IR} \leq R_{k,m}^{ER}$ ,  $R_{k,m}^s$  will be zero, and  $R_s$  is the sum of worst secrecy rate.

### C. Problem formulation

The goal of this paper is to maximize the SSR of the SWIPT-enabled NOMA system subject to the IRs' rate constraints and the ERs' harvested energy requirements. Therefore, the corresponding SSR maximization problem in the considered SWIPT-enabled NOMA system can be mathematically formulated as

$$\max_{a_m, 1 \leq m \leq M} R_s = \sum_{m=1}^M \min_k R_{k,m}^s \quad (8a)$$

$$\text{s.t.} \quad R_m^{IR} \geq Q_m, \forall m \quad (8b)$$

$$E_k^{ER} \geq E_k, \forall k \quad (8c)$$

$$\sum_{m=1}^M a_m \leq 1. \quad (8d)$$

where  $Q_m$  and  $E_k$  are the minimum data rate required by the  $m$ -th IR and the minimum harvested energy required by the  $k$ -th ER, respectively.

The considered SSR maximization problem, with power allocation through a max-min function in the presence of inter-user interference, is non-convex. The solution is therefore non-trivial and cannot be obtained directly. In order to solve this problem, one may rely on an exhaustive search method over all the possible power allocations. Nevertheless, it is obvious that this exhaustive search method incurs intensive computational complexity in the number of users (IRs and ERs). As a result, an efficient power allocation policy is proposed to achieve the maximum SSR of the SWIPT-enabled NOMA system in the following section.

### III. POWER ALLOCATION ALGORITHM

In this section, we propose an efficient power allocation scheme for the SSR maximization of the SWIPT-enabled NOMA system. In particular, we first simplify the original optimization problem and identify the feasible region of the total transmit power. The corresponding non-convex SSR maximization problem is then transformed to a sequence of convex sub-problems, which can be solved simultaneously. Finally, the optimal closed-form power allocation solution is derived with the help of KKT conditions.

#### A. Problem simplification

In order to achieve a constraint convex set of problem (8), we reformulate the constraints (8b) and (8c) as follows:

$$a_m \geq A_m \left( P|h_m|^2 \sum_{i=m+1}^M a_i + \sigma^2 \right), \forall m. \quad (9)$$

$$P \sum_{m=1}^M a_m \geq \frac{E_k}{\eta|g_k|^2}, \forall k. \quad (10)$$

where  $A_m = \frac{2^{Q_m} - 1}{P|h_m|^2}$ .

Therefore, the constraint set formed by the original constraint (8d) and the reformulated constraints (9) and (10) is convex. In order to further facilitate addressing problem (8), we propose the following theorem to simplify its objective function.

*Theorem 1:* For all IRs, the following equation holds:

$$\min_{1 \leq k \leq K} R_{k,m}^s = R_{K,m}^s, \forall m.$$

*Proof:* According to (5), we can define the function  $f(x) = \log_2 \left( 1 + \frac{Ax}{Bx + \sigma^2} \right)$ , where  $A = Pa_m$ ,  $B = P \sum_{i=m+1}^M a_i$  and  $x = |g_k|^2$ . Then the first-order derivative of  $f(x)$  on  $x$  can be derived as

$$\frac{df(x)}{dx} = \frac{A\sigma^2}{\ln 2 \left( 1 + \frac{Ax}{Bx + \sigma^2} \right) (Bx + \sigma^2)^2}. \quad (11)$$

Apparently,  $f(x)$  is a monotonically increasing function of  $x$  since  $\frac{df(x)}{dx} > 0$ . In other words, the better the channel gain  $|g_k|^2$  is, the greater  $R_{k,m}^{ER}$  is. Therefore, we can conclude that  $\min_k R_{k,m}^s = R_{K,m}^s$ . The proof is completed. ■

Let us denote the channel gains from the BS to IRs and the  $K$ -th ER with  $0 < |h_1|^2 \leq |h_2|^2 \leq \dots \leq |h_{M_k}|^2 \leq |g_K|^2 \leq |h_{M_k+1}|^2 \leq \dots \leq |h_M|^2$ . According to (4), (5) and (6), we can observe that if  $|h_m|^2 \leq |g_K|^2$ , the secrecy rate of  $m$ -th IR is zero. Therefore, the SSR of the considered SWIPT-enabled NOMA system, i.e., (6), can be rewritten as

$$R_s = \sum_{m=M_k+1}^M (R_m^{IR} - R_{K,m}^{ER}). \quad (12)$$

Now, the original SSE maximization problem in (8) can be transformed as follows:

$$\max_{a_m, 1 \leq m \leq M} R_s = \sum_{m=M_k+1}^M (R_m^{IR} - R_{K,m}^{ER}) \quad (13a)$$

$$\text{s.t.} \quad a_m \geq A_m \left( P|h_m|^2 \sum_{i=m+1}^M a_i + \sigma^2 \right), \forall m \quad (13b)$$

$$P \sum_{m=1}^M a_m \geq \frac{E_k}{\eta|g_k|^2}, \forall k \quad (13c)$$

$$\sum_{m=1}^M a_m \leq 1. \quad (13d)$$

#### B. Minimum transmit power

From the constraints (13b) and (13c), it can be observed that there exists a minimum power threshold that enables the transformed problem (13) feasible. That is, once the total transmit power  $P$  is less than this threshold, problem (13) would be infeasible. Therefore, in this section, we first identify the feasible set of the total transmit power  $P$  before addressing problem (13).

According to (13b),  $P$  should be no less than a predefined minimum power, denoted by  $P_{min\_ir}$ , to satisfy the minimum data rate requirements. This threshold can be obtained when the constraints (8b) are active, i.e.  $R_m^{IR} = Q_m, \forall m$  [28]. In particular, let  $a_m^{min}$  be the power allocation coefficient of the  $m$ -th IR at which the right-hand side (RHS) and the left-hand side (LHS) of (9) are equal, thus  $P_{min\_ir}$  can be calculated by

$$P_{min\_ir} = \sum_{m=1}^M a_m^{min} P. \quad (14)$$

It should be noted that noted that  $a_m^{min} (m \in \{1, 2, \dots, M\})$  can be determined sequentially in the order of  $M, M-1, \dots, 1$  when the inequality in (9) is set to equality.

Similarly, there is another predefined minimum power threshold at the BS, denoted by  $P_{min\_er}$ , to meet the ERs' harvested energy demands. This minimum power  $P_{min\_er}$  can be obtained when the equality in (8c) holds, i.e.  $E_k^{ER} = E_k, \forall k$ . Based on (8d) and (10), we can derive the expression of

$P_{min\_er}$  as

$$P_{min\_er} = \max_k \left\{ \frac{E_k}{\eta |g_k|^2} \right\}. \quad (15)$$

In summary, the SSR maximization problem in (8) is feasible only when the total transmit power  $P$  is no less than the minimum power  $P_{min}$  requested by the QoS constraints of IRs and the harvested energy constraints of ERs, i.e.,

$$P \geq P_{min} = \max\{P_{min\_ir}, P_{min\_er}\}. \quad (16)$$

and the achieved SSR for the considered SWIPT-enabled NOMA system is set to zero for the case of  $P < P_{min}$ .

### C. Optimal power allocation strategy

In this section, we aim to propose an optimal power allocation strategy for the SSR maximization under the given feasible set of the total transmit power  $P \geq P_{min}$ . Thus problem (13) can be further rearranged as follows:

$$\max_{a_m, 1 \leq m \leq M} R_s = \sum_{m=M_k+1}^M (R_m^{IR} - R_{K,m}^{ER}) \quad (17a)$$

$$\text{s.t. } a_m \geq A_m \left( P|h_m|^2 \sum_{i=m+1}^M a_i + \sigma^2 \right), \forall m \quad (17b)$$

$$\sum_{m=1}^M a_m \leq 1. \quad (17c)$$

In the following, we first substitute (4) and (5) into (12) and reformulate the objective function of (17) as follows:

$$R_s = \sum_{m=M_k+1}^M \left[ \log_2 \left( 1 + \frac{P|h_m|^2 a_m}{P|h_m|^2 \sum_{i=m+1}^M a_i + \sigma^2} \right) \right. \quad (18)$$

$$\left. - \log_2 \left( 1 + \frac{P|g_K|^2 a_m}{P|g_K|^2 \sum_{i=m+1}^M a_i + \sigma^2} \right) \right]$$

$$= \log_2 \left( P|h_{M_k+1}|^2 \sum_{i=M_k+1}^M a_i + \sigma^2 \right)$$

$$- \log_2 \left( P|g_K|^2 \sum_{i=M_k+1}^M a_i + \sigma^2 \right)$$

$$+ \sum_{m=M_k+1}^{M-1} \left[ \log_2 \left( P|h_{m+1}|^2 \sum_{i=m+1}^M a_i + \sigma^2 \right) \right.$$

$$\left. - \log_2 \left( P|h_m|^2 \sum_{i=m+1}^M a_i + \sigma^2 \right) \right].$$

To obtain a simplified expression of (18), we define

$$C_m \triangleq \begin{cases} P|g_K|^2, m = M_k \\ P|h_m|^2, M_k + 1 \leq m \leq M \end{cases}$$

$$t_m \triangleq \sum_{i=m+1}^M a_i, M_k \leq m \leq M-1$$

and

$$f_m(t_m) \triangleq \log_2 (C_{m+1} t_m + \sigma^2) - \log_2 (C_m t_m + \sigma^2).$$

Then, (18) can be rewritten as

$$R_s = \sum_{m=M_k}^{M-1} f_m(t_m). \quad (19)$$

From (19), it can be observed that the current objective function  $R_s$  is the sum of  $M - M_k$  subfunctions. Therefore, we can divide the optimization problem (17) into  $M - M_k$  subproblems, which are separately maximizing the  $f_m(t_m)$  for the  $m$ -th IR ( $M_k \leq m \leq M-1$ ) subject to all the constraints in (17). The optimal power allocation policy to problem (17) can be derived on a basis of the solutions to these  $M - M_k$  subproblems. In the following, we would provide a detailed solution procedure of these subproblems.

For the objective function  $f_m(t_m)$  of the  $m$ -th subproblem, we can easily obtain its first-order derivative on  $t_m$  which is shown as follows:

$$\frac{df_m(t_m)}{dt_m} = \frac{(C_{m+1} - C_m) \sigma^2}{\ln 2 (C_{m+1} t_m + \sigma^2) (C_m t_m + \sigma^2)}. \quad (20)$$

From (20), we can conclude that  $\frac{df_m(t_m)}{dt_m} \geq 0$  due to  $C_{m+1} > C_m$ . So,  $f_m(t_m)$  is a monotonically increasing function with respect to  $t_m$ . Thus, maximizing the  $f_m(t_m)$  is equivalent to maximizing the  $t_m$ . Consequently, the subproblem for maximizing the  $f_m(t_m)$  subject to the system constraints can be reformulated as follows:

$$\max_{a_m, 1 \leq m \leq M} t_m \quad (21a)$$

$$\text{s.t. } a_m \geq A_m \left( P|h_m|^2 \sum_{j=m+1}^M a_j + \sigma^2 \right), \forall m \quad (21b)$$

$$\sum_{m=1}^M a_m \leq 1. \quad (21c)$$

Moreover, the optimization problem (21) is convex. Therefore, we can invoke the KKT conditions from (21) and arrive the following expressions which enables us to find the optimal solutions to (21):

$$\lambda = \begin{cases} \mu_k - \sum_{i=1}^{k-1} \mu_i A_i P|h_i|^2, & 1 \leq k \leq m \\ \mu_k - \sum_{i=1}^{k-1} \mu_i A_i P|h_i|^2 + 1, & m < k \leq M. \end{cases} \quad (22)$$

$$\mu_i \left[ A_i \left( P|h_i|^2 \sum_{j=i+1}^M a_j + \sigma^2 \right) - a_i \right] = 0, 1 \leq i \leq M \quad (23)$$

$$\mu_i \geq 0, 1 \leq i \leq M \quad (24)$$

$$\lambda \left( \sum_{i=1}^M a_i - 1 \right) = 0 \quad (25)$$

$$\lambda \geq 0 \quad (26)$$

where  $\{\mu_i\}_{i=1}^M$  and  $\lambda$  are the Lagrange multipliers for the inequality constraints (21b) and (21c), respectively.

Motivated by the results in [28], the closed-form solution to our SSR maximization problem in (21) can be derived as

TABLE I  
OPTIMAL POWER ALLOCATION SCHEME

- 1) Initialization;
- 2) Sort the channel gains  $h_m$  and  $g_k$ , respectively;
- 3) Compute the minimum transmit power  $P_{min\_ir}$  according to (14);
- 4) Compute the minimum transmit power  $P_{min\_er}$  according to (15);
- 5) **IF**  $P < \max\{P_{min\_ir}, P_{min\_er}\}$
- 6) Infeasible;
- 7) **ELSE**
- 8) Compute  $a_m$  according to (29) for each  $m \in [1, M]$ .
- 9) **END**

follows:

$$a_i = \frac{A_i \left[ P|h_i|^2 \left( 1 - \sum_{j=1}^{i-1} a_j \right) + \sigma^2 \right]}{2Q_i}, 1 \leq i \leq m. \quad (27)$$

$$t_m = 1 - \sum_{i=1}^m a_i \quad (28)$$

According to (27), it is clear that the optimal power allocation coefficient  $a_i^*$  for the  $i$ -th IR ( $1 \leq i \leq m$ ) can be determined uniquely. Furthermore, since the equality condition holds for constraint (21c), i.e.,  $\sum_{m=1}^M a_m = 1$ , the optimal power allocation coefficient  $a_M^*$  for the  $M$ -th IR is also unique.

In summary, we have obtained the unique optimal solution to simultaneously maximize the  $f_m(t_m)$  for each IR subject to all the constraints in (17), where the problem (17) can be addressed sequentially [28]. Therefore, the optimal power allocation coefficients of each IR for maximizing the SSR of the system can be obtained by

$$a_m^* = \begin{cases} \frac{(2^{Q_m} - 1) \left[ P|h_m|^2 \left( 1 - \sum_{i=1}^{m-1} a_i^* \right) + \sigma^2 \right]}{P|h_m|^2 2^{Q_m}}, & 1 \leq m \leq M-1, \\ 1 - \sum_{i=1}^{M-1} a_i^*, & m = M. \end{cases} \quad (29)$$

#### IV. SIMULATION RESULTS AND DISCUSSION

In this section, simulation results are provided in order to validate the SSR performance of the proposed power allocation policy in the considered SWIPT-enabled NOMA systems. All the results are obtained from various random locations of the users with identical and independent Rayleigh block fading channels and Log-Normal shadowing with standard deviation of 8 dB. The path-loss exponent  $\alpha$  is set to 2.5 for a practical line-of-sight SWIPT scenario [33]. In addition, the EH efficiency is set to  $\eta = 10\%$  [34]. For simplicity purposes, all IRs and ERs are considered to have the same QoS requirements, i.e.,  $Q_m = \bar{Q}$ ,  $1 \leq m \leq M$ ,  $E_k = \bar{E}$ ,  $1 \leq k \leq K$ . Note that, as shown in Section III-B, there exists a minimum transmit power  $P_{min}$  at the BS due to the QoS constraints. Therefore, for the case of  $P < P_{min}$ , the achieved SSR  $R_s$  is set to zero. It should also be noted that these system parameters are merely chosen to demonstrate the performance

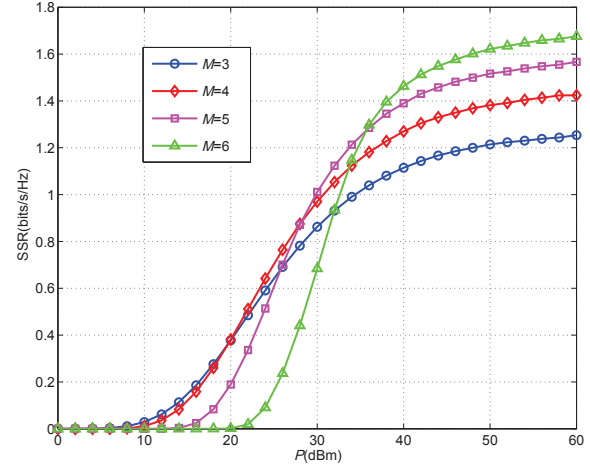


Fig. 2. SSR versus the total transmit power of the BS  $P$  for different numbers of IRs with  $\bar{Q} = 2.5$  bits/s/Hz,  $\bar{E} = -50$  dBm and  $K = 2$ .

in an example and can easily be modified to any other values depending on the specific scenario under consideration.

We first evaluate the SSR of SWIPT-enabled NOMA network as a function of the total transmit power  $P$  under different numbers of IRs. It can be seen from Fig. 2 that the SSR achieved by the proposed optimal power allocation scheme is monotonically non-decreasing with respect to  $P$ . Specifically, in the low transmit power region, the achieved SSR is zero, which is mainly due to the fact that the corresponding  $P$  does not meet the system's minimum transmit power requirement  $P_{min}$ ; once  $P > P_{min}$ , the achieved SSR is increasing as  $P$  increases. On the other hand, when  $P$  is large enough, i.e.,  $P > 36$  dBm, the SSR performance of the system becomes better with the increasing number of IRs. Although it needs more transmit power to meet the minimum QoS requirements if the number of IRs  $M$  increases, the enhanced diversity gain is capable of compensating this loss, and hence improve the overall performance.

Next, the SSR performance of the proposed optimal power allocation algorithm with various QoS demands are evaluated and shown in Fig. 3 and Fig. 4. We first investigate the impact of the minimum data rate requirement on the achieved SSR. As shown in Fig. 3, the achieved SSR decreases as  $\bar{Q}$  increases. This is because, with the increasing  $\bar{Q}$ , more transmit power would be allocated to the IRs with the poor channel conditions in order to satisfy their QoS requirements, and thus it would in turn degrade the system performance. Besides, as we expected, the more IRs exist in the network, the more quickly the achieved SSR declines. We then study the impact of the minimum harvested energy requirement  $\bar{E}$  on the achieved SSR. As it can be seen from Fig. 4, the SSR presents a decrease trend as  $\bar{E}$  increases. Moreover, the achieved SSR would gradually decrease to zero as  $\bar{E}$  becomes larger. This is mainly due to the fact that when  $\bar{E}$  is very large, the BS with given total transmit power cannot afford enough power to meet all ERs' minimum harvested energy requirements. Therefore, combining the results in Fig. 3 and Fig. 4, there is a



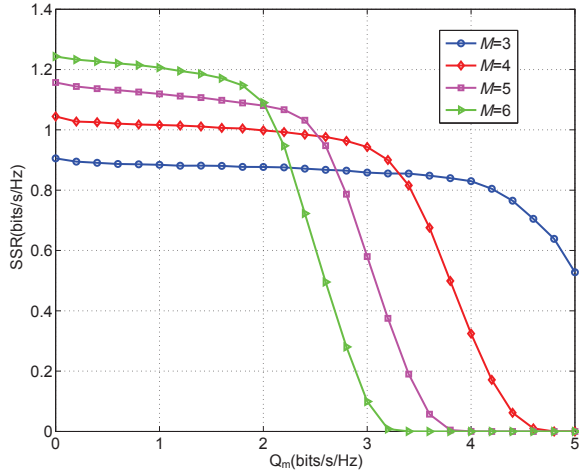


Fig. 3. SSR versus the minimum data rate requirement  $\bar{Q}$ , i.e.,  $Q_m$ , for different numbers of IRs with  $P = 30$  dBm,  $\bar{E} = -50$  dBm and  $K = 2$ .

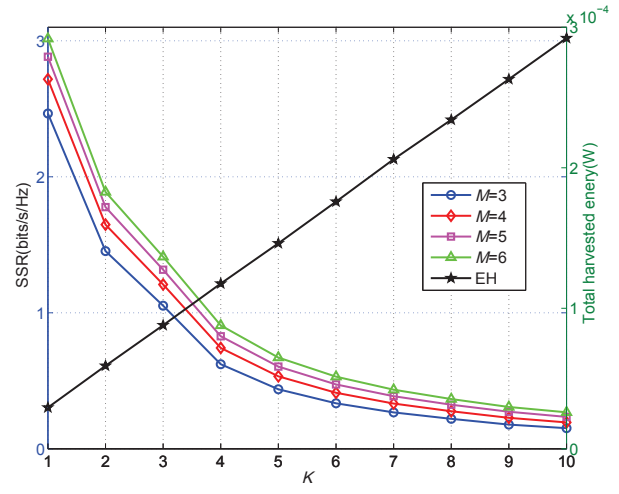


Fig. 5. SSR versus the number of ERs  $K$  for different numbers of IRs with  $P = 30$  dBm,  $\bar{Q} = 2.5$  bits/s/Hz and  $\bar{E} = -50$  dBm

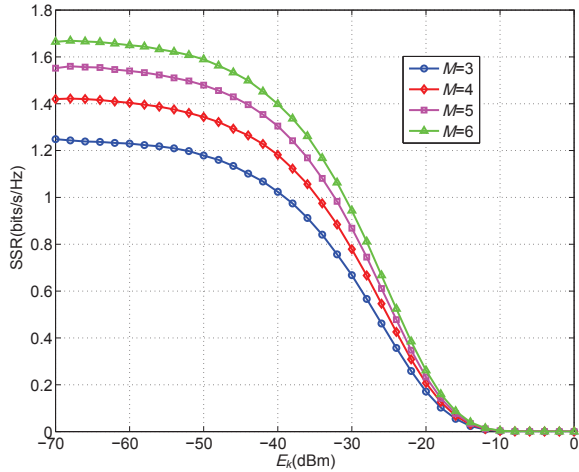


Fig. 4. SSR versus the minimum harvested energy requirement  $\bar{E}$ , i.e.,  $E_k$ , for different numbers of IRs with  $P = 30$  dBm,  $\bar{Q} = 2.5$  bits/s/Hz and  $K = 2$ .

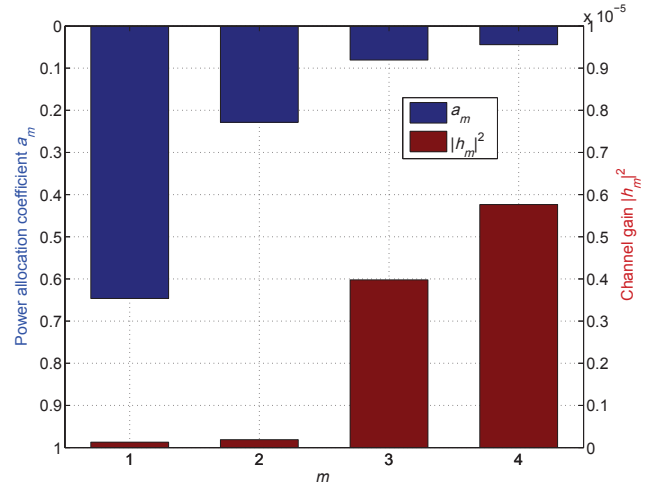


Fig. 6. Correlation between power allocation coefficient  $a_m$  and channel gain  $|h_m|^2$  with  $\bar{Q} = 1.5$  bits/s/Hz and  $M = 4$ .

balance between the individual QoS requirements of IRs and the achieved SSR, and thus the system parameters should be selected appropriated in order to achieve a good performance.

We then investigate the impact of number of ERs on the achieved SSR and the total energy harvested. As can be seen from Fig. 5, the achieved SSR decreases as the number of ERs  $K$  increases. This is because an extra diversity gain can be obtained when a larger number of ERs exists in the system, which would naturally degrade the system's SSR performance due to the eavesdropping ability. On the other hand, the total harvested energy presents a liner growth as  $K$  increases. Therefore, there exists an optimal number of ERs which depends on both the minimum harvested energy requirements and minimum rate requirements.

We also study the effect of the channel gain and the number of IRs on the selection of the optimal power allocation coefficients. The results in Fig. 6 reveal that the corresponding

power allocation coefficient is inversely proportional to the channel gain. This is because the IR with poor channel gain needs more transmit power to guarantee its minimum data rate requirement, and thus the corresponding power allocation coefficient should be increased. While in Fig. 7, it can be observed that the sum of the power allocation coefficients  $a_3$  and  $a_4$  in the system with four IRs is equal to the coefficient  $a_3$  in the system with three IRs. According to (29), the  $m$ -th IR with  $1 \leq m \leq M-1$  only needs to meet the minimum data rate requirement, while the remaining transmit power  $P - P_{min}$  would be only used for increasing the  $M$ -th IR's secrecy rate. Therefore, when  $M$  increases, the transmit power allocated to the  $M$ -th IR, i.e., that with best channel gain, would be redistributed. However, when the total transmit power  $P$  increases, more transmit power would be allocated to  $M$ -th IR, and this will raise more interference to the other IRs in return. To avoid such a situation, the power allocation policy

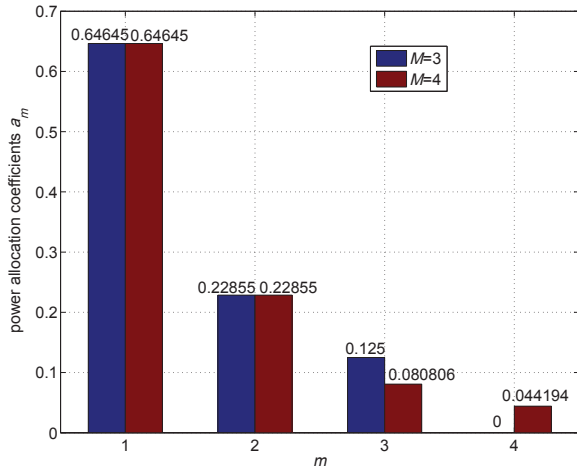


Fig. 7. Power allocation coefficient  $a_m$  versus the number of IRs  $M$  with  $P = 60$  dBm and  $\bar{Q} = 1.5$  bits/s/Hz

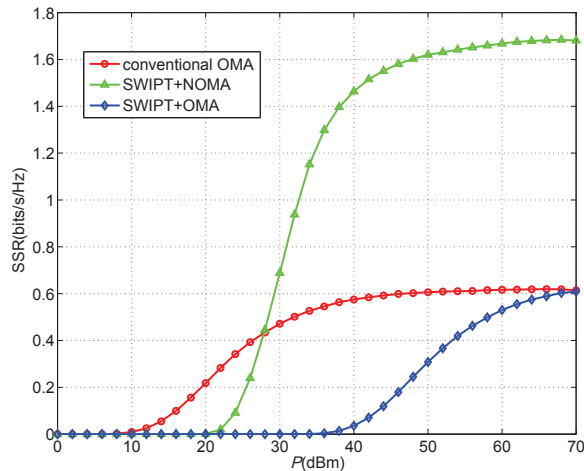


Fig. 8. SSR versus the total transmit power of the BS  $P$  for different downlink schemes with  $\bar{Q} = 2.5$  bits/s/Hz and  $\bar{E} = -50$  dBm

is almost invariable, and thus the  $M$ -th IR would only get a small increment of the transmit power when  $P$  increases.

Finally, To further verify the effectiveness of the proposed power allocation policy, we compare the SSR of the proposed algorithm (marked as 'SWIPT+NOMA') with two other downlink schemes, i.e., conventional OMA scheme and the combination of SWIPT and conventional OMA (marked as 'SWIPT+OMA'). In the conventional OMA scheme, the IRs are assumed to uniformly apportion the spectrum resource and utilize the same power allocation policy. Fig. 8 shows the SSR achieved with three aforementioned schemes versus the total transmit power of the BS  $P$ . From Fig. 8, it can be seen that, when the system has sufficient power resource, i.e.,  $P > 28$  dBm, the SSR performance of the proposed scheme is much better than those of two other schemes. On the other hand, in a low transmit power region, the conventional OMA scheme has a better SSR performance. This is because, compared

with the proposed scheme and the 'SWIPT+OMA' scheme, the conventional OMA scheme doesn't consider the minimum harvested energy requirements of ERs, which would consume part of the transmit power and thus reduce the SSR.

## V. CONCLUSION

In this paper, we have addressed the SSR maximization problem for SWIPT-enabled NOMA systems. Our target is to maximize the SSR of the system while satisfying all the IRs' and ERs' QoS demands. Due to the highly correlated variables, the SSR maximization problem is recognized as non-convex and thus difficult to obtain the optimal solution in polynomial time. In order to overcome this difficulty, we first identify the feasible set for the total transmit power with the system QoS constraints. With this set, we then transform the original non-convex problem to a sequence of convex sub-problems, where the closed-form expression of optimal power allocation policy is derived based on the KKT conditions. Numerical results demonstrate the SSR performance of the proposed strategy. More importantly, compared to the conventional OMA approach, our findings have illustrated that significant performance gains can be achieved by our proposed algorithm.

## REFERENCES

- [1] Q. C. Li, H. Niu, A. T. Papathanassiou, and G. Wu, "5G network capacity: Key elements and technologies," *IEEE Veh. Technol. Mag.*, vol. 9, pp. 71–78, Mar. 2014.
- [2] F. Boccardi, R. W. Heath, A. Lozano, T. L. Marzetta, and P. Popovski, "Five disruptive technology directions for 5G," *IEEE Commun. Mag.*, vol. 52, pp. 74–80, Feb. 2014.
- [3] L. Dai, B. Wang, Y. Yuan, S. Han, C. I. I, and Z. Wang, "Non-orthogonal multiple access for 5G: solutions, challenges, opportunities, and future research trends," *IEEE Commun. Mag.*, vol. 53, pp. 74–81, Sept. 2015.
- [4] A. Li, Y. Lan, X. Chen, and H. Jiang, "Non-orthogonal multiple access (NOMA) for future downlink radio access of 5g," *China Commun.*, vol. 12, pp. 28–37, Dec. 2015.
- [5] Y. Saito, A. Benjebbour, Y. Kishiyama, and T. Nakamura, "System-level performance evaluation of downlink non-orthogonal multiple access (NOMA)," in *2013 IEEE 24th Annual International Symposium on Personal, Indoor, and Mobile Radio Communications (PIMRC)*, pp. 611–615, Sept. 2013.
- [6] S. Timotheou and I. Krikidis, "Fairness for non-orthogonal multiple access in 5G systems," *IEEE Signal Process. Lett.*, vol. 22, pp. 1647–1651, Oct. 2015.
- [7] B. Di, L. Song, and Y. Li, "Sub-channel assignment, power allocation, and user scheduling for non-orthogonal multiple access networks," *IEEE Trans. Wireless Commun.*, vol. 15, pp. 7686–7698, Nov. 2016.
- [8] Z. Yang, Z. Ding, P. Fan, and N. Al-Dhahir, "A general power allocation scheme to guarantee quality of service in downlink and uplink NOMA systems," *IEEE Trans. Wireless Commun.*, vol. 15, pp. 7244–7257, Nov. 2016.
- [9] F. Fang, H. Zhang, J. Cheng, S. Roy, and V. C. M. Leung, "Joint user scheduling and power allocation optimization for energy-efficient NOMA systems with imperfect CSI," *IEEE J. Sel. Areas Commun.*, vol. 35, pp. 2874–2885, Dec. 2017.
- [10] J. Men, J. Ge, and C. Zhang, "Performance analysis of nonorthogonal multiple access for relaying networks over nakagami- $m$  fading channels," *IEEE Trans. Veh. Technol.*, vol. 66, pp. 1200–1208, Feb. 2017.
- [11] Q. Zhang, Q. Li, and J. Qin, "Robust beamforming for nonorthogonal multiple-access systems in MISO channels," *IEEE Trans. Veh. Technol.*, vol. 65, pp. 10231–10236, Dec. 2016.
- [12] Z. Ding, F. Adachi, and H. V. Poor, "The application of mimo to non-orthogonal multiple access," *IEEE Trans. Wireless Commun.*, vol. 15, pp. 537–552, Jan. 2016.
- [13] X. Lu, P. Wang, D. Niyato, D. I. Kim, and Z. Han, "Wireless networks with RF energy harvesting: A contemporary survey," *IEEE Commun. Surveys Tuts.*, vol. 17, pp. 757–789, Secondquarter 2015.



- [14] L. R. Varshney, "Transporting information and energy simultaneously," in *2008 IEEE International Symposium on Information Theory*, pp. 1612–1616, July 2008.
- [15] A. A. Nasir, X. Zhou, S. Durrani, and R. A. Kennedy, "Relaying protocols for wireless energy harvesting and information processing," *IEEE Trans. Wireless Commun.*, vol. 12, pp. 3622–3636, July 2013.
- [16] X. Zhou, R. Zhang, and C. K. Ho, "Wireless information and power transfer in multiuser OFDM systems," *IEEE Trans. Wireless Commun.*, vol. 13, pp. 2282–2294, Apr. 2014.
- [17] J. Xu, L. Liu, and R. Zhang, "Multiuser MISO beamforming for simultaneous wireless information and power transfer," *IEEE Trans. Signal Process.*, vol. 62, pp. 4798–4810, Sept. 2014.
- [18] J. Tang, D. K. C. So, A. Shojaefard, and K. K. Wong, "Energy efficiency optimization with SWIPT in MIMO broadcast channels for internet of things," to appear in *IEEE Internet Things J.*, 2017.
- [19] S. Zhao, Q. Li, Q. Zhang, and J. Qin, "Antenna selection for simultaneous wireless information and power transfer in MIMO systems," *IEEE Commun. Lett.*, vol. 18, pp. 789–792, May 2014.
- [20] J. Tang, D. K. C. So, A. Shojaefard, K. K. Wong, and J. Wen, "Joint antenna selection and spatial switching for energy efficient MIMO SWIPT system," *IEEE Trans. Wireless Commun.*, vol. 16, no. 7, pp. 4754–4769, July 2017.
- [21] Z. Yang, Z. Ding, P. Fan, and N. Al-Dhahir, "The impact of power allocation on cooperative non-orthogonal multiple access networks with SWIPT," *IEEE Trans. Wireless Commun.*, vol. 16, pp. 4332–4343, July 2017.
- [22] Y. Liu, Z. Ding, M. Elkashlan, and H. V. Poor, "Cooperative non-orthogonal multiple access with simultaneous wireless information and power transfer," *IEEE J. Sel. Areas Commun.*, vol. 34, pp. 938–953, Apr. 2016.
- [23] T. N. Do, D. B. da Costa, T. Q. Duong, and B. An, "Improving the performance of cell-edge users in MISO-NOMA systems using TAS and SWIPT-based cooperative transmissions," *IEEE Trans. Green Commun. Netw.*, vol. 2, pp. 49–62, Mar. 2018.
- [24] A. D. Wyner, "The wire-tap channel," *The Bell System Technical Journal*, vol. 54, pp. 1355–1387, Oct. 1975.
- [25] X. Wang, M. Tao, J. Mo, and Y. Xu, "Power and subcarrier allocation for physical-layer security in OFDMA-based broadband wireless networks," *IEEE Trans. Inf. Forensics Security*, vol. 6, pp. 693–702, Sept. 2011.
- [26] L. Liu, R. Zhang, and K. C. Chua, "Secrecy wireless information and power transfer with MISO beamforming," in *2013 IEEE Global Communications Conference (GLOBECOM)*, pp. 1831–1836, Dec. 2013.
- [27] M. Alageli, A. Ikhlef, and J. Chambers, "Optimization for maximizing sum secrecy rate in MU-MISO SWIPT systems," *IEEE Trans. Veh. Technol.*, vol. 67, pp. 537–553, Jan. 2018.
- [28] Y. Zhang, H. M. Wang, Q. Yang, and Z. Ding, "Secrecy sum rate maximization in non-orthogonal multiple access," *IEEE Commun. Lett.*, vol. 20, pp. 930–933, May 2016.
- [29] P. D. Diamantoulakis and G. K. Karagiannidis, "Maximizing proportional fairness in wireless powered communications," *IEEE Wireless Commun. Lett.*, vol. 6, pp. 202–205, Apr. 2017.
- [30] P. D. Diamantoulakis, K. N. Pappi, Z. Ding, and G. K. Karagiannidis, "Wireless-powered communications with non-orthogonal multiple access," *IEEE Trans. Wireless Commun.*, vol. 15, pp. 8422–8436, Dec. 2016.
- [31] Y. Liu, Z. Ding, M. Elkashlan, and H. V. Poor, "Cooperative non-orthogonal multiple access with simultaneous wireless information and power transfer," *IEEE J. Sel. Areas Commun.*, vol. 34, no. 4, pp. 938–953, 2015.
- [32] J. Park, B. Clerckx, C. Song, and Y. Wu, "An analysis of the optimum node density for simultaneous wireless information and power transfer in ad hoc networks," *IEEE Trans. Veh. Technol.*, vol. PP, no. 99, pp. 1–1, 2017.
- [33] IEEE P802.11 Wireless LANs, "TGn Channel Models", IEEE 802.11-03/940r4, Tech. Rep., May 2004.
- [34] I. Krikidis, S. Timotheou, S. Nikolaou, G. Zheng, D. W. K. Ng, and R. Schober, "Simultaneous wireless information and power transfer in modern communication systems," *IEEE Commun. Mag.*, vol. 52, no. 11, pp. 104–110, Nov. 2014.